



1 **Assesing the Value of High-Resolution Data and Parameters Transferability**
2 **Across Temporal Scales in Hydrological Modeling: A Case Study in Northern**
3 **China**

4

5 Mahmut Tudaji, Yi Nan*, Fuqiang Tian*

6 Department of Hydraulic Engineering & State Key Laboratory of Hydrosience and Engineering,
7 Tsinghua University, Beijing 100084, China

8 *Correspondence to:* Yi Nan (ny1209@qq.com), Fuqiang Tian (tianfq@tsinghua.edu.cn)

9 Abstract: The temporal resolution of input data and the computational time step are crucial factors
10 affecting the accuracy of hydrological model forecasts. This study presents a four-source hydrological
11 model tailored to the runoff characteristics of the mountainous areas in Northern China. Using this model,
12 along with meteorological and hydrological data from seven catchments of varying sizes in Northern
13 China, we investigated the impact of different input data resolutions and computational time steps on
14 simulation accuracy, as well as the transferability of parameters across different time scales. The results
15 show that: (1) The proposed model performs well across different spatial and temporal scales, with
16 average NSE for daily and hourly flow forecasts of 0.93 and 0.85, respectively. (2) For daily streamflow
17 simulations, there was a significant improvement in model performance when the data resolution was
18 increased from 24 hours to 12 hours; however, beyond the 12-hour resolution, the improvement became
19 negligible. For hourly streamflow simulations, the enhancement in overall flood process accuracy
20 becomes insignificant when the resolution exceeds 6 hours, although higher resolutions continue to
21 improve the precision of peak flow simulations. (3) When the computational time step is fixed (e.g., 1
22 hour), model parameters are transferable across different data resolutions; parameters calibrated with
23 daily data can be used in models driven by sub-daily data. However, parameters are not transferable when
24 the computational time step varies. Therefore, it is recommended to utilize smaller computational time
25 step when constructing hydrological models even in the absence of high-resolution input data. This
26 strategy ensures that the same simulation accuracy can be achieved while preserving the transferability
27 of model parameters, thus enhancing the robustness of the model.

28 **1 Introduction**

29 Hydrological modeling plays a critical role in water resources management, flood forecasting, and
30 climate impact assessments. Accurate simulation of runoff processes is essential for understanding water
31 balance and predicting hydrological extremes. The effectiveness of a hydrological model is influenced
32 by the scale of input data (resolution), the scale of the model's computation, and the scale of the
33 hydrological processes being modelled (López-Moreno et al., 2013; Merheb et al., 2016).

34 In the past, hydrological modeling has typically relied on daily or coarser resolution data, limiting its
35 applicability for shorter time steps required in scenarios like flash flood forecasting. Models that utilize
36 coarse or artificially enhanced data may introduce biases when applied to finer temporal scales, as they
37 may fail to accurately represent the variability and magnitude of key hydrological variables. However,
38 advancements in measurement technologies, including high-frequency automated rain/streamflow
39 gauges and phased array rain-radars, have enabled access to high-resolution rainfall and runoff datasets.



40 Despite these technological advances, the quantitative benefits of high-resolution data in enhancing
41 hydrological model performance remain unclear. For instance, studies on the impact of rainfall data
42 resolution on hydrological models have produced inconsistent results. Research such as Jaehak et al.
43 (2011) suggested that finer temporal resolution significantly improves model simulations, whereas other
44 studies (Kannan et al., 2006; Ficchi et al., 2016) found that greater data resolution does not necessarily
45 lead to better model performance. Our previous research (Tudaji et al., 2024) in southern China showed
46 that high-resolution data does not always have positive impact on model performance. Nevertheless, we
47 and other related studies acknowledge that further studies across different climate zones and models are
48 necessary to validate and extend the generality of these findings.

49 Moreover, there remain other unresolved issues regarding data resolution that warrant further
50 investigation. When a certain resolution is selected for a watershed model based on current data
51 availability (or a specific standard) and the model's parameters are calibrated accordingly, the model is
52 essentially considered constructed. However, if the resolution of future input data differs from that used
53 during the model's construction, it is uncertain whether the model's forecast results will remain reliable.
54 There is a need to explore whether the model's parameters were optimized solely to maximize simulation
55 metrics for that particular resolution, and whether these parameters can be transferred effectively across
56 different data resolutions. Reynolds et al. (2017) found that the model calibrated by the daily data
57 performance almost as good as the model calibrated by data at sub-daily resolutions. However, this
58 conclusion was reached under a fixed computational time step, and the study (including the
59 aforementioned studies on input data resolution) also acknowledges that the generality of their
60 conclusions to other regions and models warrants further investigation.

61 Similarly, another issue that arises when constructing hydrological models is the choice of the model's
62 computational time step. The time dependence and transferability of parameters has been widely studied.
63 (Krajewski et al. 1991; Finnerty et al. 1997; Littlewood and Croke 2008; Reynolds et al. 2017). Recent
64 studies have provided quantitative insights into relationship of parameters at different computation time
65 steps. Wang et al. (2009) established the relationship between the parameters and the square root of the
66 time step; Jie et al. (2017) established transformation function between parameter values at different time
67 steps. However, it remains uncertain whether a finer computational time step consistently leads to
68 improved simulation accuracy when the resolutions of input and output are fixed. Moreover, the extent
69 to which parameters can be transferred across different computational time steps without transformation
70 and the existence of an optimal computational time step that maximizes both parameter transferability
71 and model performance are still questions that warrant further investigation.

72 In light of these background, this study sought to enhance our understanding of the value of high-
73 resolution data and transferability of parameters across temporal scales in hydrological modeling based
74 on 7 small-to-medium catchments in northern China, using data resolutions ranging from 1 to 24 hours.
75 We designed two experiments focusing on the most common hydrological forecasting timescales—daily
76 and hourly, to investigate the value of the high-resolution data on hydrological modeling. Besides, two
77 further experiments, one with various data resolutions and another with various computation time steps,
78 were conducted to assess the transferability of parameters under different conditions. Specifically, this
79 study seeks to address three key questions:

80 (1) What is the necessary resolution of rainfall and streamflow data to provide reliable hourly and daily
81 streamflow simulations?

82 (2) When the computation time step is fixed as hourly, can parameters be transferred when adopting
83 different temporal resolutions of input data?



84 (3) When the temporal resolution of input data is fixed as daily, can parameters be transferred when
85 adopting different computation time steps?

86 The rest of this paper is structured as follows: Section 2 outlines the materials and methodology,
87 including the introduction of study catchments, the hydrological model used, and the experimental
88 designs. Section 3 presents the results of the experiments. Section 4 explains the role of high-resolution
89 data, discusses the transferability of parameters under different conditions, and provides insights into
90 selecting data resolution and computation time step during the modelling. Finally, Section 5 offers
91 concluding remarks and limitations in this study.

92 **2 Materials and methodology**

93 **2.1 Study area and data**

94 The Chaobai River, located in northern China and flowing through Beijing, is one of the five major rivers
95 in the Haihe River system of China. In this study, we utilized a set of 7 various size of catchments in the
96 upper reaches of the Chaobai River as the study area (Figure1, Table1), where data quality is relatively
97 high and human activities (such as reservoirs or dams) have minimal impact. Among them, the Xitaizi
98 Basin, the smallest one, is a hydrological experimental catchment. The other six study catchments are
99 the control regions of important hydrological stations located upstream of reservoirs or lakes on the major
100 tributaries in the upper reaches of the Chaobai River Basin.

101 The study area is characterized by a temperate monsoon climate, with precipitation highly seasonal and
102 primarily concentrated in July and August, resulting in significant seasonal and interannual variations in
103 river flow. During periods outside the rainy season, the flow is minimal, and in some cases, the river may
104 even run dry. Therefore, we chose the 2021 flood season, which saw significant flood events and has
105 relatively complete data, as the study period for this study.

106 The streamflow and rainfall data were obtained from the Rain and Hydrological Database of Beijing,
107 curated by the Beijing Hydrological Station. When selecting the above-mentioned hydrological stations
108 as the outlets for the study basins, the following principles were followed: (1) The station must have
109 discharge data with a resolution finer than hourly during flood events; (2) The upstream control area of
110 the station should be free of water control structures such as reservoirs, dams, or lakes that could
111 significantly affect the natural progression of floods; and (3) The study catchments should cover a range
112 of different scales, from a few square kilometers to several thousand square kilometers. The selection of
113 rainfall data followed similar principles, ensuring that each rain gauge station provided complete rainfall
114 data with a resolution finer than hourly throughout the entire storm runoff process. We identified 56 high-
115 quality stations situated within the study catchments from the database. The number of rainfall gauges
116 per catchment varied from 1 to 14, averaging 8 stations. Additionally, the rainfall gauging area—
117 calculated as the catchment area divided by the number of stations—ranged from 3 km² to 373 km², with
118 an average of 157 km². The Thiessen Polygon method (Han and Bray, 2006) was employed to generate
119 the areal rainfall data for each sub-basin in each catchment.

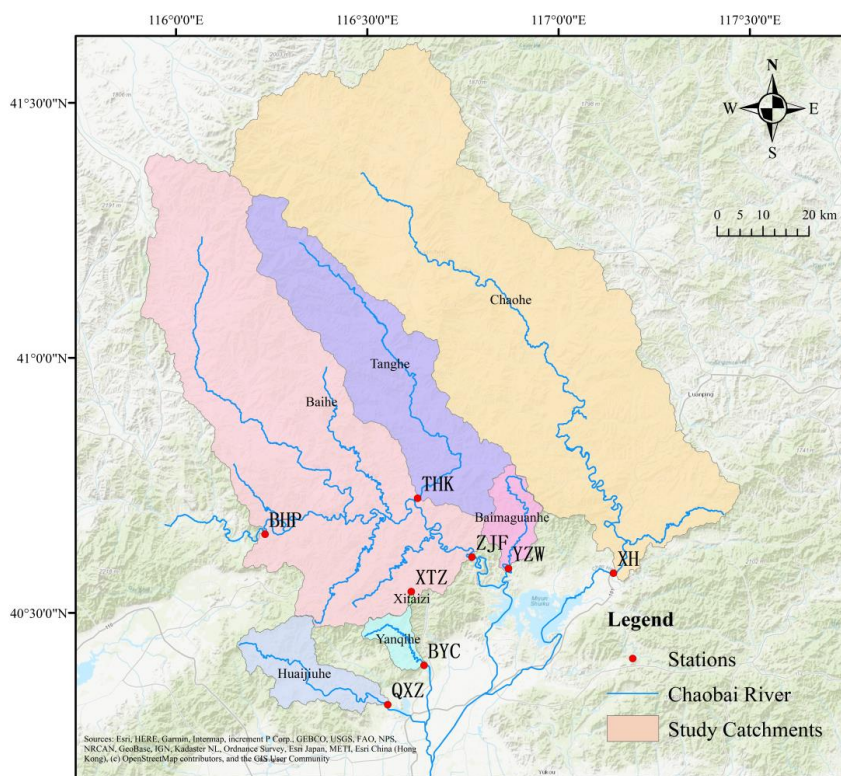


Figure 1: Geographic distribution of study catchments

Table 1. Information of study catchments and data

NO.	Basin	Hydrological Station	Abbr.	Drainage area (km ²)	Number of rainfall gauges	Rainfall gauging area (km ²)
1	Xitaizi	Xitaizi	XTZ	3.11	1	3.11
2	Yanqihe	Baiyachang	BYC	96.06	6	16.01
3	Baimaguanhe	Yaoziwa	YZW	180.04	8	22.51
4	Huaijiuhe	Qianxinzhuang	QXZ	332.85	10	33.29
5	Tanghe	Tanghekou	THK	1263.13	4	315.78
6	Baihe	Zhangjiafen	ZJF	4660.91	14	332.92
7	Chaohe	Xiahui	XH	4845.98	13	372.77

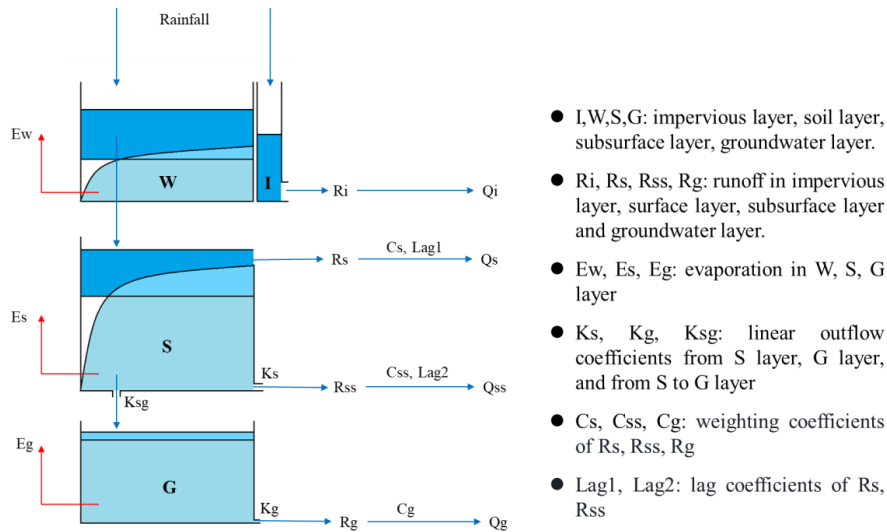
120
121
122

123 2.2 Hydrological model

124 The study catchments are located in a rocky mountainous region with severe weathering and high
 125 vegetation cover (Zheng et al., 2013; Yu et al., 2017). On the basis of intensive hydrological and isotopic
 126 observations from the Xitaizi experimental catchment, Zhao et al (2019) found that preferential flow in
 127 the heavily weathered granite and shallow soils makes up the majority of the stormflow. Recent studies
 128 also indicate that subsurface flow is a significant contributor to flood generation (Addisie et al., 2020;
 129 Xiao et al., 2020; Wang et al., 2022). To effectively capture the hydrological processes within the study



130 area, a four-source hydrological model was developed, designed to represent multiple hydrological
 131 pathways. The model's structural diagram (Figure 2) illustrates these pathways, where the I layer denotes
 132 the impervious layer, which occupies a small and relatively constant proportion in the study area. The W
 133 layer represents the soil moisture storage layer, which is responsible for simulating the soil moisture
 134 content. The S layer signifies the shallow subsurface layer, encompassing both the soil runoff layer and
 135 the weathered bedrock; when the S layer gets saturated, it generates surface runoff (Rs), which, along
 136 with subsurface runoff (Rss), constitutes the primary sources of stormflow. Lastly, the G layer represents
 137 the deep groundwater layer, which is the main contributor to baseflow. The equations for structure the
 138 model was listed in Appendix A.
 139



140
 141 **Figure 2: The structural diagram of the hydrological model**
 142 The routing process is modeled using the Muskingum method (McCarthy, 1938; Cunge, 1969), with the
 143 equation given as:
 144
$$Q_{i+1}^{t+1} = C_1 Q_i^t + C_2 Q_i^{t+1} + C_3 Q_{i+1}^t + (C_1 + C_2) Q_L$$
 (1)
 145 where i is spatial index, t is temporal index, and Q_L is lateral flow.
 146 In the Muskingum method, the three parameters C_1 , C_2 , C_3 must satisfy the conditions of being within
 147 the 0-1 range and their sum equaling 1. To accommodate these constraints within automatic parameter
 148 optimization algorithms, this study reparametrizes the model by optimizing the values of C_1+C_2 and $C_1/$
 149 (C_1+C_2) , thereby determining the optimal values for the original parameters.

150 2.3 Experimental design for the value of high-resolution data

151 Daily streamflow and hourly streamflow are important modeling targets in hydrological research and
 152 practice. To test the value of rainfall and measured streamflow data at different resolutions for simulating
 153 streamflow at these two scales, we designed two specific experiments: the daily modeling test and the
 154 hourly modeling test. In this context, 'daily' and 'hourly' refer to the target time scales for the model's
 155 predictions. The flowchart of the tests was shown as Figure 3, and the details are as follows.
 156 (1) Daily modeling test: This test was designed to investigate the impact of high-resolution rainfall data
 157 on daily streamflow simulation. The model was driven by rainfall data at various resolutions (ranging



158 from 1h to 24h) and calibrated using daily resolution streamflow data. This setup aimed to assess whether
159 (and to what extent) sub-daily rainfall data can enhance daily streamflow simulation.

160 (2) Hourly modeling test: This test was designed to investigate the impact of high-resolution input and
161 streamflow data on hourly streamflow simulation. In this test, the temporal resolutions of input rainfall
162 data and calibration streamflow data were the same, both set as various resolutions (ranging from 1h to
163 24h). The model was calibrated using streamflow data with the given temporal resolution, and then the
164 hourly streamflow simulated by the calibrated model was evaluated based on the hourly measured
165 streamflow. This setup aimed to determine the necessary data resolution for providing reliable hourly
166 streamflow simulation.

167 These experiments aimed to investigate how data resolution affects the accuracy and reliability of
168 streamflow predictions across various temporal scales. To minimize potential impacts from varying
169 computational time steps, the hydrological simulations were consistently set to a 1-hour time step for
170 both tests. This standardization was maintained across all cases, with different input data resolutions used.
171 Specifically, all input data, including rainfall, were resampled to a 1-hour resolution via prior averaging
172 before driving the model. As a result, the model's original outputs were always produced at an hourly
173 scale.

174 In the daily modeling test, rainfall data at varying temporal scales was input into the hydrological model
175 to produce simulated hourly streamflow, which was later aggregated to the daily scale for comparison
176 with observed daily streamflow. Model parameters were then optimized by aligning the simulation with
177 observations using Python Surrogate Optimization Toolbox (pySOT, Eriksson et al., 2019), aiming to
178 maximize the Nash-Sutcliffe efficiency (NSE). The optimization process, iterated via Symmetric Latin
179 Hypercube Design (SLHD), concluded upon convergence or after reaching a 3000-iteration threshold.
180 After 100 trials, the final parameters were selected based on maximum NSE. Additionally, after
181 calibration, Relative Error of Peak flow (REP) was computed as a secondary performance metric. These
182 metrics were calculated as follows:

$$183 \quad NSE = 1 - \frac{\sum_{t=1}^n (Q_t^{obs} - Q_t^{sim})}{\sum_{t=1}^n (Q_t^{obs} - \overline{Q^{obs}})} \quad (2)$$

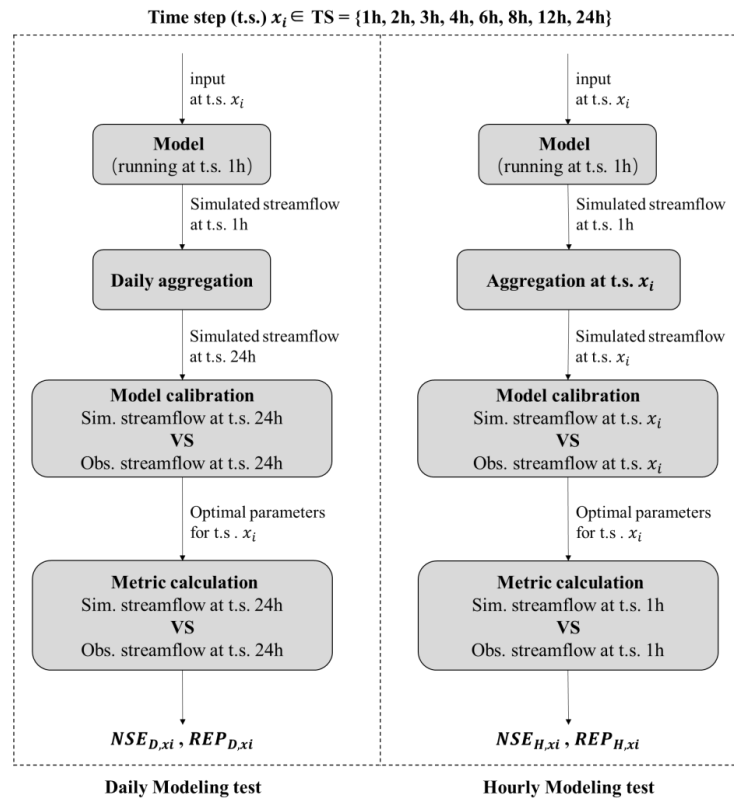
$$184 \quad REP = \frac{Q_{sim,p} - Q_{obs,p}}{Q_{obs,p}} \quad (3)$$

185 where, Q_t^{obs} and Q_t^{sim} are the streamflow for the observed and simulated time series, $\overline{Q^{obs}}$ is the
186 average value of the observed streamflow, $Q_{sim,p}$ and $Q_{obs,p}$ are the simulated and observed peak flow,
187 respectively.

188 The hourly modeling test followed a similar procedure to the daily modeling test, inputting rainfall data
189 at various temporal resolutions into the hydrological model to produce simulated hourly streamflow. This
190 output was aggregated to match the resolution of the input data and compared with the corresponding
191 observed data for calibration. The performance of calibrated model on simulating hourly streamflow was
192 then assessed by calculating NSE and REP, based on the hourly simulated and observed streamflow data.
193 The flowchart of the experimental tests was illustrated in Figure 3, where D and H refer to daily and
194 hourly test, x_i is each member of the time step (t.s.) set (TS), which consists of 1h, 2h, 3h, 4h, 6h, 12h
195 and 24h. NSE_{D,x_i} and REP_{D,x_i} are the NSE of and REP of daily streamflow forced by rainfall at time
196 step of x_i . Similarly, NSE_{H,x_i} and REP_{H,x_i} denote the NSE and REP for hourly streamflow at time step
197 of x_i .



198 After tests, the paired two-sample t-test, a widely used statistical method to determine whether the means
 199 of two related groups of samples are significantly different (e.g., Xu et al., 2017), was adopted to test
 200 whether the performance of the hydrological model based on high-resolution data was significantly
 201 improved.



202

203

Figure 3: Flowchart of the daily modeling and hourly modeling tests

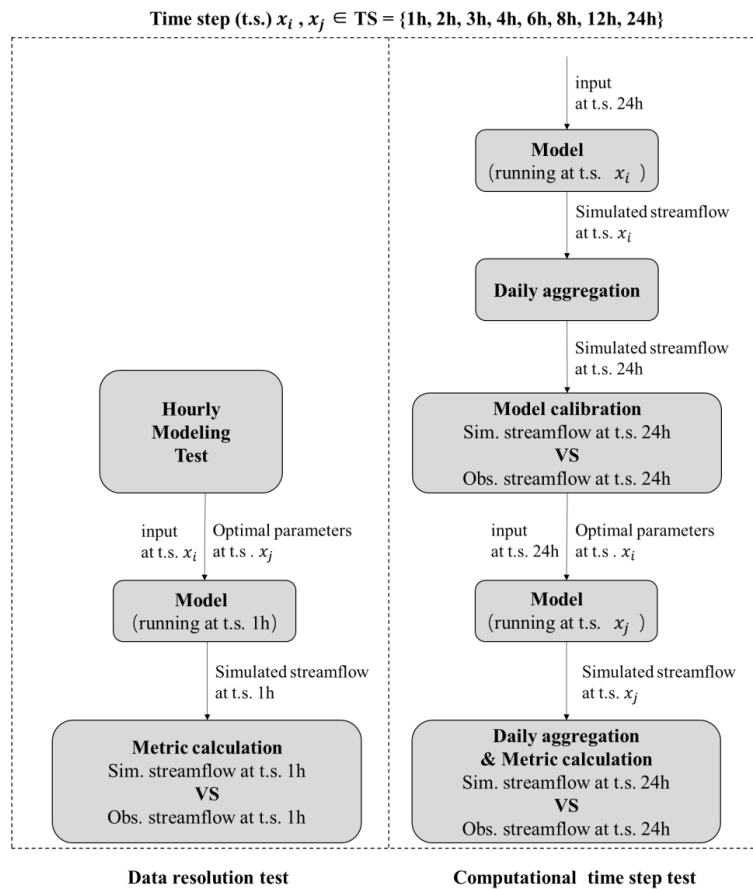
204 **2.4 Experimental design for parameters transferability**

205 To test the potential impact of the resolution of training data and the computational time step on
 206 calibration of model parameters, as well as the transferability of these parameters across different time
 207 scales, we designed two tests: the data resolution test and the computational timestep test. The flowchart
 208 of the tests was shown as Figure 4, and the details are as follows.

209 (1) Data resolution test: in this test, the model's computational time step was fixed as 1 hour, while the
 210 temporal resolution of the input and measured streamflow varied from 1 hour to 24 hours (as in the hourly
 211 test). Previously, optimal parameter sets, Par_{x_i} , have been obtained under varying resolutions (x_i) of
 212 input and measured streamflow data in hourly modeling tests. In this data resolution test, the optimal
 213 parameter set obtained at one resolution (referred to as the pre-transfer resolution) was used to drive the
 214 model with input data at another resolution (referred to as the post-transfer resolution), resulting in hourly
 215 simulated streamflow. The simulation accuracy, measured by NSE, was then calculated. By comparing



216 the changes in the simulation metrics obtained by a same set of parameters and different input resolutions,
 217 the transferability of the parameters across varying resolutions was tested.
 218 (2) Computational time step test: in this test, the model's computational time step varied from 1 hour to
 219 24 hours, while the temporal resolution of the input rainfall and measured streamflow data was fixed as
 220 24 hours. Firstly, input data at the resolution of 24 hours was fed into the model, and the model was run
 221 at varied time steps, resulting simulated streamflow at varied time steps. Next, the simulated streamflow
 222 was aggregated in daily, and the model parameters were calibrated based on observed daily streamflow.
 223 In this way, the model parameters under different computational steps are obtained. Then, the optimal
 224 parameter set obtained at one computational time step (referred to as the pre-transfer computational time
 225 step) was used to drive the model at another computational time step (referred to as the post-transfer
 226 computational time step), and the NSE was calculated based on the simulated daily streamflow obtained
 227 at this time step. By comparing the changes in simulation metrics, the transferability of parameters
 228 obtained at one computational time step to another was tested.



229
 230

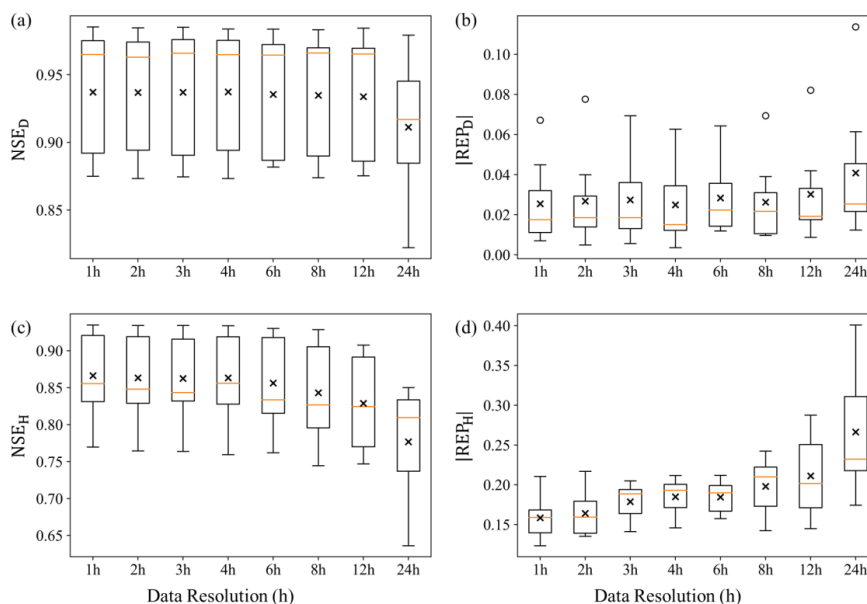
Figure 4: Flowchart of the data resolution and computational time step tests



231 **3 Results**

232 **3.1 The value of high-resolution data**

233 The results of the daily and the hourly modeling tests are shown in Figure 5. Subplots (a) and (b) represent
 234 the NSE and absolute values of REP in the daily modeling test, respectively. Subplots (c) and (d) depict
 235 these two metrics in the hourly modeling test. In the daily test, the average NSE obtained by various data
 236 resolutions varied in the range of 0.91 - 0.94. The model performed worst when using 24-hour resolution
 237 data, but even then, the lowest NSE value was 0.82 in the Yanqihe catchment at BYC station, and in the
 238 other 6 catchments, the NSE exceeded 0.89. As for REP, the average $|REP_D|$ at various data resolutions
 239 ranged between 2% and 4% indicating high accuracy in simulation on peak flow at daily scale. In the
 240 hourly modeling test, the metrics got slightly worse compared with the daily test. The average NSE across
 241 various data resolutions ranged from 0.78 to 0.87. The model performed worst when using 24h resolution
 242 data, with the lowest NSE of 0.64, but the NSE exceeds 0.8 in five of the study catchments. The model
 243 produced NSE higher than 0.83 in 6 catchments when using 1h rainfall and streamflow data. The average
 244 $|REP_H|$ varied in the range of 16% - 27%. Compared to the daily modeling test, the model's accuracy in
 245 simulating peak flow declined noticeably in hourly modeling, as the evaluation is more strict. Overall,
 246 these results demonstrated the high performance and reliability of the model in these catchments, with
 247 high NSE and low $|REP|$.



248

249 **Figure 5: Box plot of NSE, $|REP|$ in the daily and the hourly modeling tests across 7 catchments**

250 In both daily and hourly modeling tests, there was an obvious improvement in model performance when
 251 the data resolution increased. For instance, in the daily modeling test, when the data resolution shifted
 252 from 24h to sub-daily 12h, the average NSE increased from 0.91 to 0.93 and the average $|REP|$ decreased
 253 from 4.08% to 3.02%. In the hourly modeling test, the improvement was more obvious. The average
 254 NSE increased from 0.78 to 0.83 and the average $|REP|$ decreased from 27% to 21%, when the data



255 resolution shifted from 24h to sub-daily 12h. But such improvement got increasingly limited as the
 256 resolution further increased.

257 To quantify the difference in the model performances when adopting data with different resolutions,
 258 paired two-sample t-tests were conducted, and the results are shown in Table 2. In the daily modeling
 259 test, significant improvement (at 0.05 significance level) on streamflow simulation was brought by sub-
 260 daily (1h – 12h) resolution rainfall data compared to the daily data, as indicated by the low p values in
 261 the last row of Table 2a and Table 2b. However, compared to 12h resolution, only the 1-hour resolution
 262 brought a significant improvement in NSE at the significance level of 0.05. As for |REP|, there were
 263 significant differences in |REP| at 2h and 8h resolution compared to 12h resolution. Overall, the results
 264 suggested that for daily streamflow forecasting, continuously increasing rainfall data resolution beyond
 265 the 12h threshold did not bring significant improvement on model performance. That is, the simulated
 266 daily streamflow obtained from a model driven by 12h rainfall input had comparable reliability to that
 267 forced by 1h data, and the effect of rainfall data with a temporal resolution exceeding 12h on enhancing
 268 daily forecasted flow was negligible.

269 Similar results were observed in the hourly modeling test (Table 2c and Table 2d). Compared to the daily
 270 data, utilizing higher-resolution data effectively enhanced the model's forecasting performance for hourly
 271 streamflow. Specifically, regarding the NSE, there were significant differences in the model's
 272 performance when using 8h resolution data compared to that obtained by 2h to 6h resolution data. But,
 273 when the data resolution reached 6 hours or higher, there were no statistically significant differences in
 274 NSEs, indicating that further increasing the resolution did not consistently enhance overall simulation
 275 accuracy. Consequently, taking NSE as the performance metric, simulated hourly streamflow obtained
 276 by a model driven and calibrated by 6h data was comparably accurate to that obtained by higher
 277 resolution data. Data with a resolution higher than 6h did not provide significant additional value.
 278 Compared to NSE, the improvement in |REP| was more pronounced with the increase in data resolution
 279 in the hourly modeling test. Compared with daily (24h) resolution data, all sub-daily resolution (1h-12h)
 280 data showed significant improvement in |REP| (at 0.05 significance level). Comparing the effects of sub-
 281 daily scale data, although there was no significant difference in the |REP| when resolutions were close
 282 (e.g., 6-hour and 8h resolutions), significant differences in |REP| still existed when the resolution was
 283 sufficiently high (e.g., 1h) compared to other resolutions. For instance, the first column of Table 2d
 284 indicated that only the |REP| obtained with 2h resolution data showed no statistically significant
 285 difference when compared to 1h resolution data. This suggests that continuously increasing data
 286 resolution has greater value in improving the accuracy of predictions on peak flow.

287 **Table 2 P-values of the paired two-sample t-tests for each metric**

288 **Table 2a P-values of the paired two-sample t-tests for NSE in daily modeling test**

Resolution	1h	2h	3h	4h	6h	8h	12h
2h	0.987						
3h	0.932	0.962					
4h	0.459	0.562	0.693				
6h	0.033*	0.175	0.043*	0.054			
8h	0.223	0.330	0.109	0.157	0.770		
12h	0.041*	0.095	0.148	0.061	0.537	0.599	
24h	0.036*	0.042*	0.031*	0.036*	0.039*	0.031*	0.046*

289 **Table 2b P-values of the paired two-sample t-tests for |REP| in daily modeling test**



Resolution	1h	2h	3h	4h	6h	8h	12h
2h	0.5581						
3h	0.1446	0.8063					
4h	0.6260	0.8122	0.3503				
6h	0.3196	0.9739	0.7922	0.6138			
8h	0.8420	0.6117	0.4098	0.8532	0.3476		
12h	0.0743	0.0164*	0.2985	0.1927	0.2364	0.0412*	
24h	0.0314*	0.0189*	0.0490*	0.0582	0.0763	0.0352*	0.0497*

290 **Table 2c P-values of the paired two-sample t-tests for NSE in hourly modeling test**

Resolution	1h	2h	3h	4h	6h	8h	12h
2h	0.368						
3h	0.283	0.571					
4h	0.370	0.666	0.559				
6h	0.088	0.044*	0.109	0.096			
8h	0.037*	0.017*	0.032*	0.028*	0.016*		
12h	0.013*	0.007*	0.010*	0.011*	0.007*	0.028*	
24h	0.009**	0.007**	0.008**	0.009**	0.008**	0.011*	0.011*

291 **Table 2d P-values of the paired two-sample t-tests for |REP| in hourly modeling test**

Resolution	1h	2h	3h	4h	6h	8h	12h
2h	0.327						
3h	0.006**	0.084					
4h	0.001**	0.009*	0.194				
6h	0.000**	0.001**	0.113	0.378			
8h	0.005**	0.006*	0.145	0.123	0.411		
12h	0.018*	0.023*	0.066	0.066	0.149	0.112	
24h	0.011*	0.015*	0.018*	0.020*	0.036*	0.031*	0.016*

292 Note: ** and * indicates significance at 0.01 and 0.05

293 3.2 Parameters transferability across data resolutions

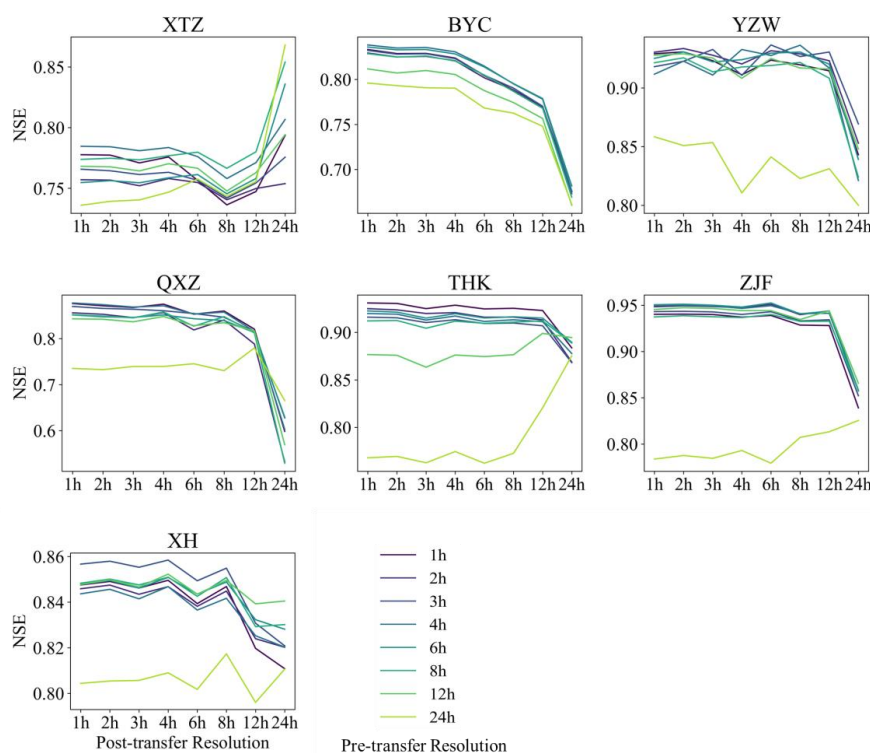
294 The optimized model parameters at various data resolutions were obtained under a fixed computational
 295 time step of 1-hour in the hourly modeling test. To assess the transferability of these parameters under
 296 different data resolutions, the data resolution test was conducted following the experimental design
 297 outlined in Section 2.4. The results are shown in Figure 6. In each subplot, each curve represents the NSE
 298 values obtained when the optimal parameters calibrated from a specific input resolution are transferred
 299 (without any transformation) to drive the model with other input resolutions.

300 First, when examining the differences among the curves, it was found that in most catchments, the curve
 301 representing the 24h resolution consistently fell below the others. This aligns with the results from the
 302 previous section, indicating that the model's performance was the lowest when using 24h resolution
 303 rainfall and streamflow data. When these parameters are transferred to other resolutions, they also
 304 exhibited the lowest performance.

305 In all catchments except for XTZ, when parameters calibrated with a specific data resolution were
 306 transferred to other resolutions, simulation accuracy improved as the resolution of the data used increased.



307 Notably, when the resolution increased from 24h to 12h, the NSE showed the most significant
 308 improvement. However, when the input data resolution ranged between 1h and 8h, the NSE remained
 309 relatively stable. This observation is consistent with the results and conclusions from Section 3.1. Even
 310 though there were some variations in model performance when parameters were transferred to other time
 311 scales, the performance remained acceptable, with the lowest NSE still exceeding 0.5. This lowest NSE
 312 occurred at the QXZ station when the pre-transfer resolution is 6h and post-transfer resolution is 24h.
 313 When the post-transfer resolution was finer than 24h, the NSE at QXZ was consistently above 0.7.
 314 Overall, after parameter transfer, the model continues to demonstrate satisfactory simulation performance.
 315



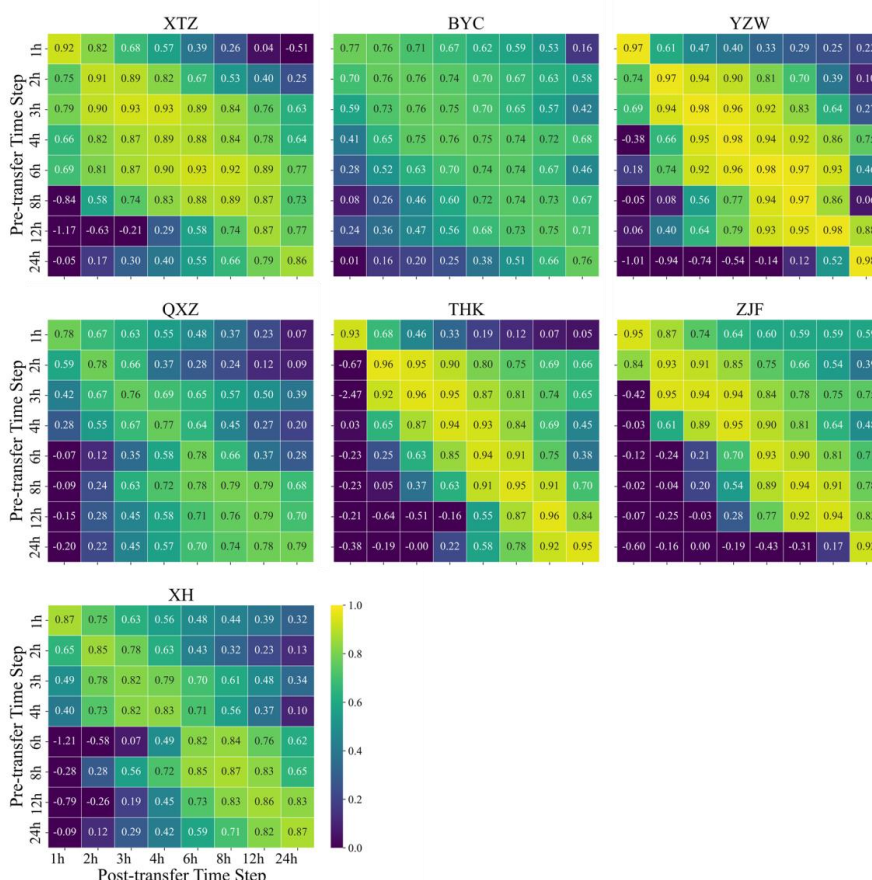
316
 317 **Figure 6: The NSE values after transferring the parameters obtained at one resolution to other resolutions**

318 3.3 Parameters transferability across computational time steps

319 To assess the transferability of parameters under different computational time steps, the computational
 320 time step test was conducted following the experimental design outlined in Section 2.4. The results are
 321 shown in Figure 7. The value in the row i and column j represents the NSE value obtained when
 322 transferring the parameters calibrated with a computation time step of x_i directly to a model with a
 323 computation time step of x_j ($x_i, x_j \in \{1h, 2h, 3h, 4h, 6h, 8h, 12h, 24h\}$, referred to as pre-transfer and
 324 post-transfer computational time step, respectively). The values on the diagonal represent the NSE values
 325 obtained when running the model with a specific computational time step and calibrating the parameters
 326 with daily streamflow. In this case, the parameters were not transferred (i.e., the pre-transfer and post-
 327 transfer time steps are the same). First, the values on the diagonal are all greater than 0.7, with most



328 exceeding 0.85, and the average is 0.88. This indicates that the model performs well across different
 329 computation time steps, further confirming its reliability. Secondly, within each basin, the values on the
 330 diagonal are very close to each other, implying that when both the input rainfall data resolution and the
 331 output streamflow resolution are at the daily scale, nearly identical simulation accuracy can be achieved
 332 regardless of the computation time step used (within the 1h-24h range).
 333 When parameters calibrated at one computation time step were transferred to other computation time
 334 steps (values in the same row in the Figure 7), the NSE values varied significantly. Compared to the
 335 results with the data resolution test in Section 3.2, the variation in NSE under the varying computation
 336 time step was much greater. In many cases, the NSE value after transferring parameters was even less
 337 than 0, indicating that the model parameters lose their transferability (with unreliable accuracy) when the
 338 model's computation time step is varied. Notably, in each subfigure, the values in the lower left part are
 339 even lower than those in the upper right part, suggesting that the model's performance is particularly
 340 unreliable when parameters calibrated at larger computation time steps are transferred to smaller ones.
 341



342
 343 **Figure 7: NSE values after transferring the parameters obtained at one computation time step to other time**
 344 **steps.**



345 **4 Discussion**

346 **4.1 Potential factors for the limited impact of high-resolution data**

347 The results indicated that increasing input data resolution, especially from 24 to 12 hours, significantly
348 boosted simulation accuracy for daily streamflow, consistent with expectations regarding the benefits of
349 high-resolution data. However, beyond the 12-hour mark, performance became marginal or even
350 declined. Similar patterns emerged in hourly simulations, where benefits of finer-than-6-hour data were
351 negligible or negative, contradicting the intuitive expectations that higher-resolution data always
352 enhances hydrological models. Similar findings were reported by previous studies that investigated the
353 effects of temporal resolution on hydrological models across different regions and model types. Ficchi
354 et al. (2016) explored 240 catchments in France using the GR4 rainfall-runoff model across eight
355 temporal scales, ranging from 6 minutes to 1 day. Their analysis revealed that, on average, finer
356 resolution data provided no additional value when model outputs were aggregated to a 6-hour reference
357 scale. Similarly, Reynolds et al. (2017), while calibrating the HBV model in two small Central American
358 basins, observed that using daily streamflow data produced results comparable to those obtained with
359 sub-daily resolution.

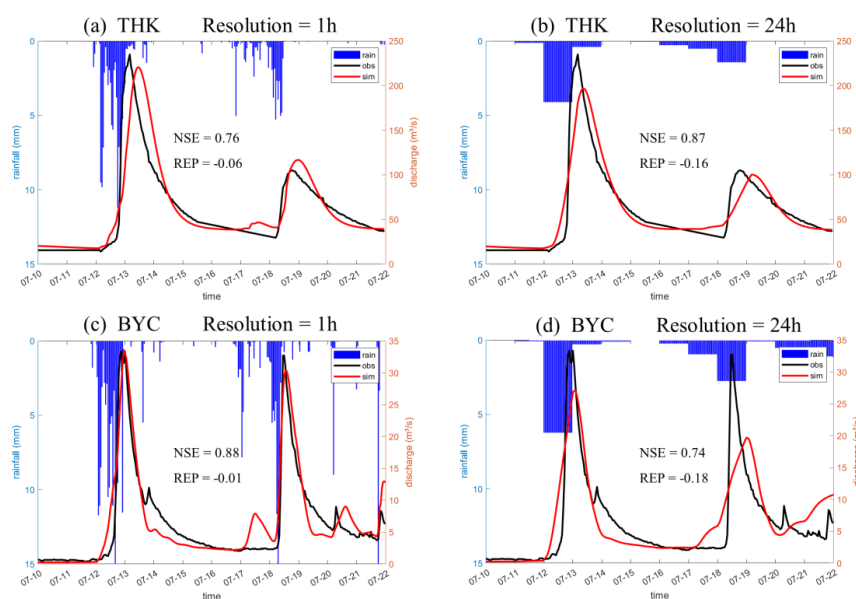
360 While the catchments and models vary across different studies, the overall findings are largely consistent,
361 suggesting that simply increasing data resolution doesn't always lead to better model performance.
362 Several factors may limit the additional benefits of higher resolution data. Firstly, a straightforward
363 reason could be the choice of the evaluation metric. In the hourly modeling test, when the resolution
364 exceeded 6 hours, there was no significant improvement in the NSE, but the |REP| showed a marked
365 change. In some cases, different metrics may conflict with each other, making it impossible to optimize
366 them simultaneously. Secondly, due to spatial and temporal autocorrelation in variables like rainfall and
367 runoff, increasing resolution beyond a certain threshold may not provide effective new information.
368 There may be no significant difference between actual high-resolution data and high-resolution data
369 obtained by resampling from coarser data. The extent of this difference is related to the characteristics of
370 the climate of the catchment and its runoff generation processes. Thirdly, model input data, particularly
371 rainfall, may have a lower signal-to-noise ratio at higher temporal resolutions due to difficulties in data
372 validation and increased uncertainty in areal average rainfall estimates (Ficchi et al., 2016; Moulin et al.,
373 2009). Besides, since hydrological models inherently simplify natural processes, they may dampen the
374 natural smoothing effect seen in rainfall-runoff interactions. As a result, using high-resolution temporal
375 data to drive the model could introduce excessive variability in the simulated flow, potentially degrading
376 the model's performance. Finally, the model's structure might not be adequately designed to handle the
377 added complexity that comes with shorter time steps. Melsen et al. (2016) pointed out that calibration
378 and validation time intervals should align with the spatial resolution to accurately capture the relevant
379 processes. Some empirical formulas within the model may not be applicable at shorter time scales.

380 **4.2 Further explanation of the transferability of parameters**

381 The results in Section 3.2 indicated that when the computation time step is fixed at 1-hour, the model
382 demonstrated good performance even when parameters are transferred to input conditions with different
383 resolutions. As shown in Figure 6, in most cases, as the input resolution improved, the NSE also increased.
384 However, some exceptions were found. At hydrological stations such as the THK and ZJF, when using
385 parameters calibrated with 24-hour data, there was an increase in NSE as the rainfall resolution decreased.



386 At the XTZ station, NSE also increased when the rainfall resolution dropped below 8 hours, regardless
 387 of the parameters used. This anomaly was particularly pronounced at the THK station. Conversely, at the
 388 BYC station, the NSE consistently decreased as the rainfall resolution decreased across all parameters.
 389 We selected the THK and BYC stations as representative cases and compared the streamflow processes
 390 driven by 1h and 24h rainfall resolutions using parameters calibrated with 24h data (as shown in Figure
 391 8). Based on these flow processes, we explored the reasons behind these observed phenomena.
 392



393
 394 **Figure 8: streamflow processes at THK and BYC driven by 1h and 24h rainfall resolutions using**
 395 **parameters calibrated by 24h data**

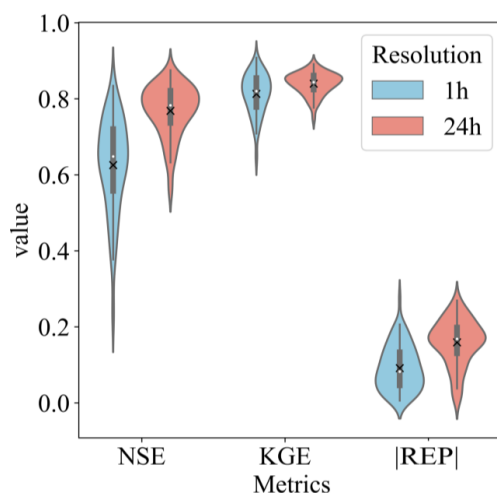
396 In Figures 8(a) and (b), the model parameters were calibrated using 24h data, but the rainfall data used
 397 to drive the model were at resolutions of 1h and 24h, respectively. The same setup was applied in Figures
 398 8(c) and (d). We observed that when using 1h resolution rainfall data, the simulated value of the first
 399 flood peak at the THK station was closer to the measured value, even though the NSE at 1h resolution
 400 was statistically lower than the NSE at 24h resolution.

401 To more comprehensively evaluate the simulation accuracy and the impact of different parameters, we
 402 conducted further analysis. As mentioned in Section 2.2, we ran 100 iterations using the pySOT program
 403 for parameter calibration, which resulted in 100 sets of optimized parameters. Using these 100 parameter
 404 sets and the rainfall data at both 1h and 24h resolutions, we evaluated the simulation accuracy of the
 405 THK station's streamflow using NSE, KGE, and REP indicators, as shown in Figure 9.

406 Among the results obtained using the 100 sets of optimal parameters, the NSE values driven by 1h
 407 resolution rainfall data were generally lower than those driven by 24h resolution rainfall, with average
 408 values of 0.63 and 0.77, respectively. The KGE values were relatively close under both resolutions, with
 409 average values of 0.81 and 0.84, respectively. As for the |REP| indicator, the trend was reversed, with the
 410 1h resolution rainfall data yielding better results than the 24h resolution data, with average |REP|
 411 values of 9% and 16%, respectively. Based on the runoff processes shown in Figure 8 and the different indicators
 412 in Figure 9, we infer that the observed phenomenon, where simulation accuracy decreases as resolution



413 increases, may be related to the evaluation metrics used and the flood characteristics of the basin.
 414 Compared to the BYC station, the THK station exhibited a slower streamflow process during flood events,
 415 particularly during the recession phase. We defined a concept similar to half-life period, denoted as T_{hl} ,
 416 to characterize the rate of flood recession. T_{hl} is the time taken for the streamflow to decay from its peak
 417 to half of the peak value. At the THK station, T_{hl} is 16 hours, while at the BYC station, T_{hl} is 8 hours,
 418 indicating that the flood recession at THK is slower than at BYC. In catchments with a more gradual
 419 recession, observed streamflow at a 24h resolution does not provide as much effective information for
 420 model's calibration as higher-resolution data. Furthermore, when 24h resolution rainfall is used as input
 421 and 1h as the computational time step, the model tends to produce a smoother simulated streamflow
 422 process, since it distributes the rainfall evenly over each hour. Consequently, parameters related to flow
 423 routing are not accurately calibrated. As a result, when the model is driven by higher resolution rainfall
 424 data such as 1h, larger errors occur in the predicted peak time. However, when using 24h resolution
 425 rainfall data, the smoothing effect of the 1h computational time step leads to a simulated recession
 426 process that more closely matches the observed values, thus improving the NSE.
 427



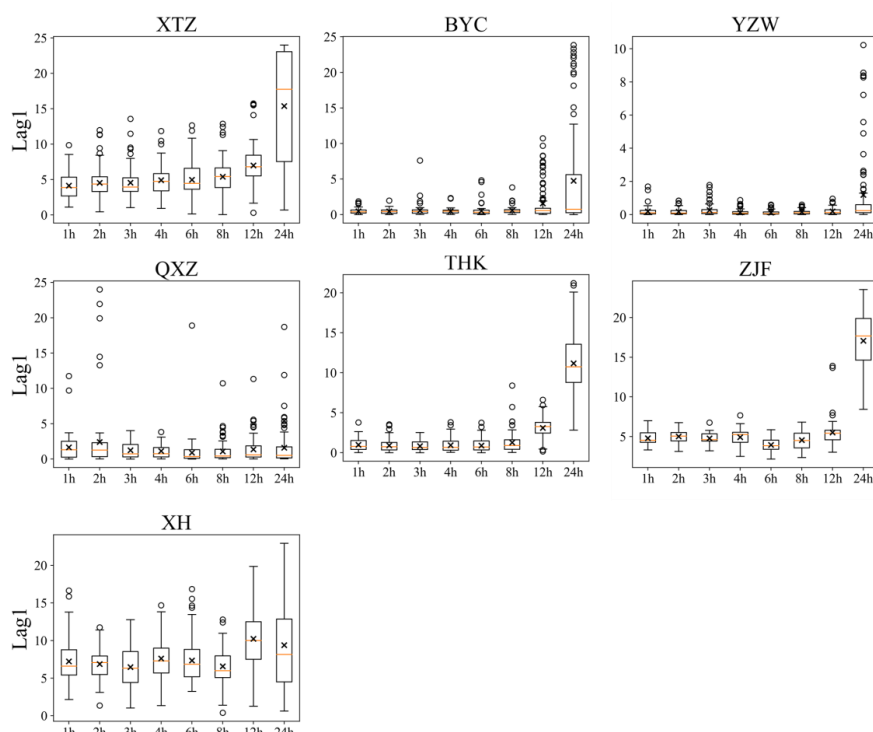
428

429 **Figure 9: Metrics at THK station using 100 sets of parameters and different resolutions of rainfall**

430 The results indicated that when the computational time step is fixed as 1h, parameters calibrated under
 431 different data resolutions can be transferred and used in models with other resolutions. To further explain
 432 the transferability of parameters and identify any patterns as resolution changes, we compared parameters
 433 across different resolutions. However, due to the parameter equifinality (Her and Chaubey, 2015; Foulon
 434 and Rousseau, 2018), a single optimal parameter set may not be representative enough to accurately
 435 reflect the patterns. Therefore, we analyzed 100 sets of parameters calibrated at each resolution, with
 436 partial results shown in Figures 10-12. The findings revealed that most parameters did not exhibit a
 437 significant and consistent trend of variation with changes in resolution. In other words, parameters
 438 calibrated under different resolutions showed little variability, which explains their transferability across
 439 resolutions. However, some parameters did show a certain consistent trend with resolution changes.
 440 Figure 10 illustrates the trend of the parameter Lag1 with changes in resolution. This parameter in the
 441 model reflects the lag time of surface runoff (the time from the generation of surface runoff until it



442 reaches the outlet of the sub-basin). As the resolution becomes coarser (from 1h to 24h), the effective
 443 information provided by the observed streamflow to the model decreases, and the requirement for
 444 precision in peak time also reduces. This relaxation in constraints led to an increase in both the mean
 445 value and the range of variation of Lag1. Notably, at stations XTZ, THK, and ZJF, when the data
 446 resolution is 24h, the mean value of Lag1 exceeds 10h or even 15h, showing a significant difference from
 447 the value at 1h resolution. In contrast, at stations BYC, YZW, and QXZ, when the data resolution is 24h,
 448 the mean value of Lag1 is less than 5h, which is not significantly different from the value at 1h resolution.
 449 This also validates the previous explanation for why the NSE at stations like THK decreases as resolution
 450 improves.

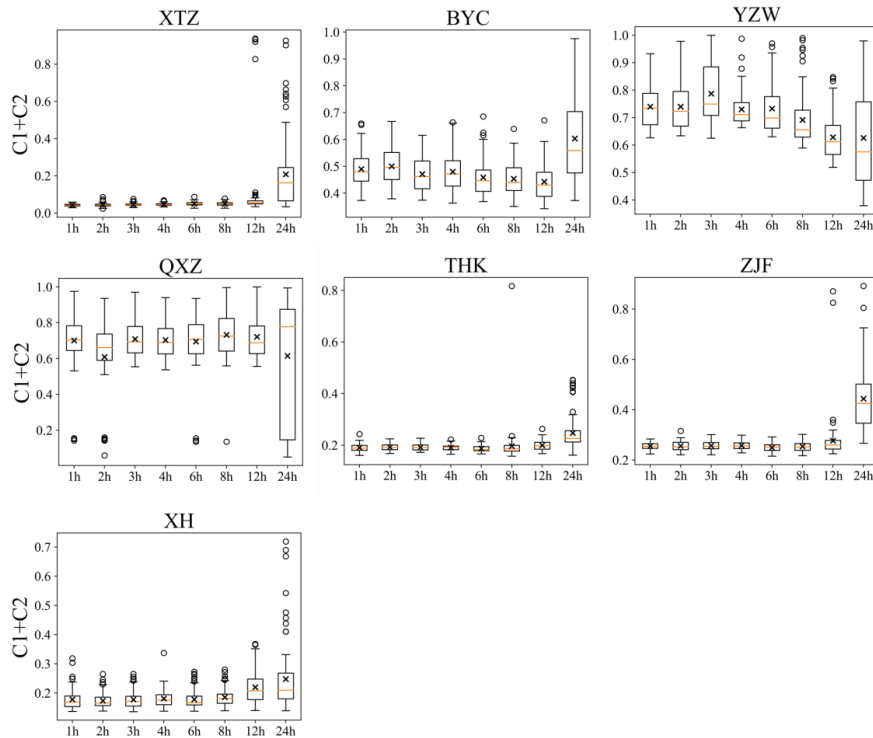


451

452

Figure 10: optimized values of Lag1 across various resolutions

453 The parameter C_1+C_2 also exhibited a regular trend of variation with changes in resolution (Figure 11).
 454 Generally, the larger this parameter, the faster the model's runoff responds to rainfall, resulting in a flood
 455 process that rises and falls sharply. When the time resolution is coarse, the variability of runoff may not
 456 be fully captured in the observed data. As a result, a model calibrated by a coarser resolution data tend
 457 to produce a smoother streamflow process. This is evident at stations such as YZW and QXZ, where the
 458 optimized C_1+C_2 value decreased as the resolution became coarser. However, we also observed that at
 459 most stations, including XTZ, THK, ZJF and XH, this parameter increased as the resolution became
 460 coarser. This may be due to the model's computational time step of 1h; when driven by coarse-resolution
 461 data, the input data are averaged over each hour, causing the runoff to be smoothed. Consequently, a
 462 larger C_1+C_2 value was selected by the parameter optimization algorithm to counterbalance this excessive
 463 smoothing.



464
 465

Figure 11: optimized values of C_1+C_2 across various resolutions

466 Besides, in certain catchments, specific parameters exhibited regular changes across varying resolutions.
 467 At BYC station, the parameter K_{sg} decreased as the resolution became coarser. K_{sg} represents the ratio
 468 of water transfer from the shallow subsurface layer to the deep groundwater layer. A decrease in K_{sg}
 469 would lead to the shallow subsurface layer becoming saturated more easily, resulting in more surface
 470 runoff. Similarly, at YZW station, the parameter K_g decreased with coarser resolution. K_g represents the
 471 ratio of water conversion from the groundwater layer to groundwater runoff. A reduction in K_g would
 472 cause the groundwater layer to saturate more readily, also indirectly leading to increased surface runoff.
 473 The 1h computational time step evenly distribute rainfall under coarse resolution, which reduces the
 474 simulated peak runoff compared to the actual peak. Therefore, the lower K_{sg} and K_g values improve
 475 simulation accuracy under coarse resolution conditions by increasing surface runoff.

476
 477

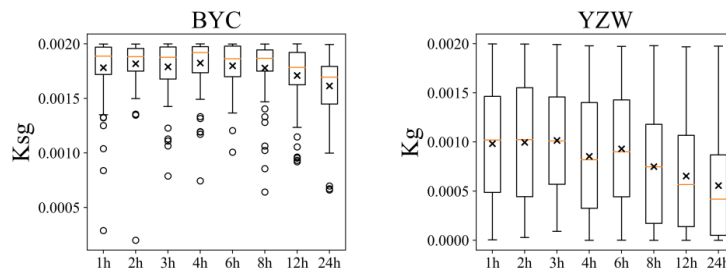


Figure 12: optimized values of K_{sg} at BYC station and K_g in YZW station across various resolutions



478 **4.3 Implications for the selection of data resolution and computation time step**

479 The findings of this study offer several key insights for building hydrological models with limited data.
480 1) Data Resolution Considerations:
481 For daily runoff simulations, it is found that a data resolution of 12h is sufficient to provide accurate
482 simulation results with relatively high precision. This suggests that higher resolution data may not yield
483 significant additional benefits for daily scale modeling. However, for hourly runoff simulations, the
484 adequacy of data resolution depends on the specific objectives of the simulation. If the primary focus is
485 on capturing the overall flood process, such as total runoff volume and approximate duration, a 6h
486 resolution is adequate. On the other hand, if the simulation aims to achieve higher accuracy in peak flow
487 estimation, employing data with finer temporal resolution can enhance the precision of these predictions.
488 This offers practical insights for building numerical models and establishing monitoring stations,
489 suggesting that high-resolution monitoring may not always be necessary. It is essential to balance the
490 additional information gained from higher resolution against the associated costs, aligning with our
491 objectives, enabling efficient resource allocation and ensuring that expenditures yield valuable returns.
492 2) Selection of Computational Time Step:
493 Regardless of whether the model is intended for daily or hourly runoff simulations, and irrespective of
494 the input data resolution, it is advisable to adopt a smaller computational time step when constructing the
495 model. This is because the results showed that the simulation accuracy on the coarse scale (24h) with
496 different computation time steps is almost the same, while the model running at a smaller computation
497 step can produce results on a finer scale, which provides the possibility for further analysis. And the
498 model's performance is particularly unreliable when parameters calibrated at larger computation time
499 steps are transferred to smaller ones. This approach also ensures that the model parameters remain
500 applicable across different data resolutions, thereby enhancing the model's flexibility and enabling it to
501 generate accurate simulation results across a range of temporal scales. With the appropriate spatial scale
502 and sufficient computational capacity, opting for a lower computational time step can make the model
503 better equipped to maintain robust performance under varying input conditions and produce results at
504 more time scales, which is crucial for ensuring the transferability of the model parameters and achieving
505 consistent results.

506 **5 Conclusions**

507 **5.1 Summary**

508 This study assessed the value of different resolution data for daily and hourly streamflow simulations
509 utilizing meteorological and runoff data with resolutions ranging from 1 hour to 24 hours from 7 small-
510 to-medium-scale catchments in northern China. Additionally, the transferability of model parameters
511 across varying data resolutions and computation time steps were investigated. Key findings are
512 summarized as follows:
513 1) For both daily and hourly streamflow simulations, utilizing sub-daily resolution rainfall and
514 streamflow data leads to substantial improvements in model performance compared with the using of the
515 daily data. However, further enhancements in data resolution yield diminishing returns. Specifically, for
516 daily streamflow simulations, improvements in model performance become negligible when the
517 resolution exceeds 12 hours. As for hourly streamflow simulations, improvements in overall flood



518 process accuracy become negligible when the resolution exceeds 6 hours, while higher resolutions further
519 enhance the precision of peak flow predictions.

520 2) When the model's computation time step is fixed at 1h, most parameters, are generally independent of
521 the input data resolution. Even when using model parameters obtained from daily data, utilizing sub-
522 daily resolution data helps improve the accuracy of hourly streamflow simulations. Conversely, when
523 the computation time step varies, the model parameters are not applicable for direct transfer to other time
524 steps. In particular, the performance of the model deteriorates more when the computation time step is
525 shifted from large to small.

526 3) It is recommended to utilize smaller computational time step when constructing hydrological models
527 even in the absence of high-resolution input data. This strategy ensures that the same prediction accuracy
528 is achieved while preserving the transferability of model parameters, thus enhancing the robustness of
529 the model.

530 **5.2 Limitations and further research needs**

531 While this study has provided valuable insights into the impacts of data temporal resolution and
532 computational time step on hydrological models, several limitations should be acknowledged. First, this
533 study focuses on a specific geographical area in Northern China and covers a limited temporal range.
534 The findings, therefore, may not be fully generalizable to other regions with different climatic,
535 hydrological, or geological conditions. Further studies across various regions and under different
536 hydrological conditions are necessary to validate and extend the applicability of these results. Second,
537 the study's conclusions are drawn based on a particular hydrological model and specific parameter
538 settings. Other models or configurations might exhibit different sensitivities to data resolution and
539 computational time step. Therefore, the generalization of these findings to other hydrological models
540 should be approached with caution. Next, results showed that the benefit of high-resolution
541 rainfall/streamflow data to daily and hourly streamflow simulation was negligible when the temporal
542 resolution was higher than a threshold, and the possible mechanism of such phenomenon was primarily
543 discussed according to the variation of runoff process and some parameters under different conditions
544 and other existing literatures. However, a deeper analysis and validation on such threshold effect are still
545 lacking, which needs further investigation. Last, the number of iterations for the optimization algorithm
546 during the model calibration process was limited. Although our previous modeling and calibration
547 practices (e.g., Nan and Tian, 2024a, 2024b) demonstrated that the current number of iterations is
548 sufficient to produce a good simulation, it does not guarantee the discovery of a globally optimal result.
549 Consequently, it is challenging to determine whether the slight decline in model performance in certain
550 catchments is due to the high-resolution data or the influence of local optima.

551
552 *Competing interests.* At least one of the (co)-authors is a member of the editorial board of Hydrology
553 and Earth System Sciences.

554

555 *Acknowledgements.* This study was made possible through the generous financial support from the
556 National Key Research and Development Program of China under grant number 2022YFC3002900,



557 National Natural Science Foundation of China under grant number 52309023 and China Postdoctoral
 558 Science Foundation under grant number 2024T170488.

559 *Code and data availability.* The data and the code of the model used in this study are available by
 560 contacting the authors.

561

562 *Author contributions.* YN and FT conceived the idea; MT and YN conducted analysis; FT provided
 563 comments on the analysis; and all the authors contributed to writing and revisions.

564 **Appendix A: List of equations for structure the model light in this study**

565 Evaporation equations:

$$566 E_w = PET * K_{ew} \quad (A1)$$

567 where PET is the mean potential evapotranspiration of the basin, E_w is the actual
 568 evaporation in W layer, K_{ew} is the linear coefficient. E_s , E_g are calculated by similar equations
 569 with the linear coefficients of K_{es} , K_{eg} .

570 Runoff equations:

$$571 WMM = WM * (1+B) \quad (A2)$$

$$572 A = WMM \left[1 - \left(1 - \frac{W}{WMM} \right)^{\frac{1}{1+B}} \right] \quad (A3)$$

$$573 R = P - E_w + W - WM, \quad \text{if } P - E_w + A \geq WMM \quad (A4)$$

$$574 R = P - E_w + W - WM \left[1 - \left(1 - \frac{P - E_w + A}{WMM} \right)^{1+B} \right], \quad \text{if } P - E_w + A < WMM \quad (A5)$$

$$575 SMM = SM * (1+EX) \quad (A6)$$

$$576 AU = SMM \left[1 - \left(1 - \frac{S}{SMM} \right)^{\frac{1}{1+EX}} \right] \quad (A7)$$

$$577 RS = R + S - SM, \quad \text{if } R + AU \geq SMM \quad (A8)$$

$$578 RS = R + S - SM \times \left[1 - \left(1 - \frac{R + AU}{SMM} \right)^{1+EX} \right], \quad \text{if } R + AU < SMM \quad (A9)$$

$$579 R_{ss} = S * K_{ss} \quad (A9)$$

$$580 R_g = G * K_g \quad (A10)$$

$$581 R_i = P \quad (A11)$$

582 where WM, SM, B and EX are storage of W, S layer and their exponential coefficients.

583 Routing equations:

$$584 Q_{i,t} = R_{i,t} * Area * imp/dT \quad (A12)$$

$$585 Q_{s,t} = [R_{s,t-1-lag1} * Cs + R_{s,t-lag1} * (1 - Cs)] * Area * (1 - imp)/dT \quad (A13)$$

$$586 Q_{ss,t} = [R_{ss,t-1-lag2} * C_{ss} + R_{ss,t-lag2} * (1 - C_{ss})] * Area * (1 - imp)/dT \quad (A14)$$

$$587 Q_{g,t} = [R_{g,t-1} * C_g + R_{g,t} * (1 - C_g)] * Area * (1 - imp)/dT \quad (A15)$$

588 where *Area* is the area of the basin, *imp* is the proportion of impervious area, and dT is the
 589 calculation time step.



590 **References**

- 591 Addisie M B, Ayele G K, Hailu N, et al. Connecting hillslope and runoff generation processes in the
592 Ethiopian Highlands: The Ene-Chilala watershed[J]. *Journal of Hydrology and Hydromechanics*,
593 2020, 68(4): 313-327.
- 594 Cunge, J., 1969. On the subject of a flood propagation computation method (Muskingum method).
595 *Journal of Hydraulic Research*, 7, 205–230.
- 596 Eriksson, D., Bindel, D., and A. Shoemaker, C.: pySOT and POAP: An event-driven asynchronous
597 framework for surrogate optimization, Arxiv, arXiv:1908.00420, 2019.
- 598 Ficchi A, Perrin C, Andréassian V. Impact of temporal resolution of inputs on hydrological model
599 performance: An analysis based on 2400 flood events[J]. *Journal of hydrology*, 2016, 538: 454-470.
- 600 Finnerty BD, Smith MB, Seo DJ, Koren V, Moglen GE (1997) Space-time scale sensitivity of the
601 Sacramento model to radar-gage precipitation inputs. *J Hydrol* 203(1):21–38
- 602 Foulon É, Rousseau A N. Equifinality and automatic calibration: What is the impact of hypothesizing an
603 optimal parameter set on modelled hydrological processes?[J]. *Canadian Water Resources*
604 *Journal/Revue canadienne des ressources hydriques*, 2018, 43(1): 47-67.
- 605 Han D, Bray M. Automated Thiessen polygon generation[J]. *Water resources research*, 2006, 42(11).
- 606 Her Y, Chaubey I. Impact of the numbers of observations and calibration parameters on equifinality,
607 model performance, and output and parameter uncertainty[J]. *Hydrological Processes*, 2015, 29(19):
608 4220-4237.
- 609 Jaehak J, Kannan N, Jeff G A, et al. Development of sub-daily erosion and sediment transport algorithms
610 for SWAT [J]. *Transactions of the Asabe*, 2011,54(5):1685-1691.
- 611 Jie M X, Chen H, Xu C Y, et al. Transferability of conceptual hydrological models across temporal
612 resolutions: approach and application[J]. *Water Resources Management*, 2018, 32: 1367-1381.
- 613 Kannan N, White S M, Fred W, et al. Sensitivity analysis and identification of the best evapotranspiration
614 and runoff options for hydrological modelling in SWAT-2000 [J]. *Journal of Hydrology*,
615 2006,332(3/4):456-466.
- 616 Krajewski WF, Lakshmi V, Georgakakos KP, Jain SC (1991) A monte carlo study of rainfall sampling
617 effect on a distributed catchment model. *Water Resour Res* 27(1):119–128
- 618 Littlewood IG, Croke BF (2008) Data time-step dependency of conceptual rainfall-streamflow model
619 parameters: an empirical study with implications for regionalisation. *Hydrolog Sci J* 53(4):685–695
- 620 López-Moreno J I, Vicente-Serrano S M, Zabalza J, et al. Hydrological response to climate variability at
621 different time scales: A study in the Ebro basin[J]. *Journal of hydrology*, 2013, 477: 175-188.
- 622 McCarthy, G.T., 1938. The unit hydrograph and flood routing. In *Proceedings of the Conference of North*
623 *Atlantic Division, US Engineer Department, New London, CN*, 608–609.
- 624 Melsen, L. A., Teuling, A. J., Torfs, P. J. J. F., Uijlenhoet, R., Mizukami, N., and Clark, M. P.: HESS
625 Opinions: The need for process-based evaluation of large-domain hyper-resolution models,
626 *Hydrology and Earth System Sciences*, 20, 1069-1079, 10.5194/hess-20-1069-2016, 2016.
- 627 Merheb M, Moussa R, Abdallah C, et al. Hydrological response characteristics of Mediterranean
628 catchments at different time scales: a meta-analysis[J]. *Hydrological Sciences Journal*, 2016, 61(14):
629 2520-2539.
- 630 Moulin L, Gaume E, Obled C. Uncertainties on mean areal precipitation: assessment and impact on
631 streamflow simulations[J]. *Hydrology and Earth System Sciences*, 2009, 13(2): 99-114.
- 632 Nan, Y. and Tian, F.: Glaciers determine the sensitivity of hydrological processes to perturbed climate in



- 633 a large mountainous basin on the Tibetan Plateau, *Hydrology and Earth System Sciences*, 28, 669-
634 689, 10.5194/hess-28-669-2024, 2024.
- 635 Nan, Y. and Tian, F.: Isotope data-constrained hydrological model improves soil moisture simulation and
636 runoff source apportionment, *Journal of Hydrology*, 633, 10.1016/j.jhydrol.2024.131006, 2024.
- 637 Reynolds J E, Halldin S, Xu C Y, et al. Sub-daily runoff predictions using parameters calibrated on the
638 basis of data with a daily temporal resolution[J]. *Journal of hydrology*, 2017, 550: 399-411.
- 639 Tudaji, M., Nan, Y., and Tian, F.: Assessing the value of high-resolution rainfall and streamflow data for
640 hydrological modeling: An analysis based on 63 catchments in southeast China, *EGUsphere*
641 [preprint], <https://doi.org/10.5194/egusphere-2024-1438>, 2024.
- 642 Wang S, Yan Y, Fu Z, et al. Rainfall-runoff characteristics and their threshold behaviors on a karst
643 hillslope in a peak-cluster depression region[J]. *Journal of Hydrology*, 2022, 605, 127370.
- 644 Wang Y, He B, Takase K (2009) Effects of temporal resolution on hydrological model parameters and its
645 impact on prediction of river discharge. *Hydrolog Sci J*:886–898
- 646 Xiao X, Zhang F, Li X, et al. Using stable isotopes to identify major flow pathways in a permafrost
647 influenced alpine meadow hillslope during summer rainfall period[J]. *Hydrological Processes*, 2020,
648 34(5): 1104-1116.
- 649 Xu, M., Fralick, D., Zheng, J. Z., Wang, B., Tu, X. M., and Feng, C.: The Differences and Similarities
650 Between Two-Sample T-Test and Paired T-Test, *Shanghai archives of psychiatry*, 29, 184-188,
651 10.11919/j.issn.1002-0829.217070, 2017.
- 652 Yu Y, Song X, Zhang Y, et al. Impact of reclaimed water in the watercourse of Huai River on groundwater
653 from Chaobai River basin, Northern China[J]. *Frontiers of earth science*, 2017, 11: 643-659.
- 654 ZHAO S, HU H, HARMAN C J, et al. Understanding of Storm Runoff Generation in a Weathered,
655 Fractured Granitoid Headwater Catchment in Northern China [J]. *Water*, 2019, 11: 123.
- 656 Zheng J, Yu X, Deng W, et al. Sensitivity of land-use change to streamflow in Chaobai river basin[J].
657 *Journal of Hydrologic Engineering*, 2013, 18(4): 457-464.